



25<sup>th</sup> ABCM International Congress of Mechanical Engineering  
October 20-25, 2019, Uberlândia, MG, Brazil

## Identification of the fault parameters in a rotor system by Bayesian inference with polynomial chaos expansion

**Gabriel Yuji Garoli**  
**Diogo Stuani Alves**  
**Felipe Wenzel da Silva Tuckmantel**  
**Katia Lucchesi Cavalca**  
**Helio Fiori de Castro**

School of Mechanical Engineering - University of Campinas

yujigaroli@fem.unicamp.br; dsalves@fem.unicamp.br; felipewst@fem.unicamp.br; katia@fem.unicamp.br; heliofc@fem.unicamp.br

**Abstract.** Rotor machines are vastly used in the industry. This kind of machine are subject to faults, which should be correctly identified so the right maintenance can be applied. There are different methods to identify the parameters of these faults. The rotor system may have more than one fault, which makes the identification methods more complex. Therefore, it is proposed a stochastic approach to the identification of the fault parameters. The Bayesian Inference is used. The solution of the inference is commonly made by a Monte Carlo via Markov Chains methods, but it has a high computational cost. The generalized Polynomial Chaos Expansion with the Stochastic Collocation can solve the inference and converge in a shorter time. The method approximate part of the inference by a polynomial series. This way, it resumes the problem into evaluate the expansion coefficients, which is done by the Stochastic Collocation. In this work, the Bayesian Inference is used to identify the parameters of the unbalance and misalignment present in a rotor system. This method shows satisfactory results evaluating the parameters when only one fault is present. It is expected that the method can identify the parameters for the case with two faults.

**Keywords:** Rotordynamics, Bayesian Inference, generalized Polynomial Chaos Expansion, Unbalance, Misalignment

### 1. INTRODUCTION

Rotor machines are susceptible to different types of faults, being two typical fault sources the unbalanced mass and misalignment. Due to the importance of this kind of machinery, reliable models are needed, so these faults can be identified and properly corrected.

A useful way to identify the fault parameters is by using statistical methods, such as the Bayesian Inference. Monte Carlo method via Markov Chain (MCMC) is commonly used to solve the inference. However, depending on the number of parameters of interest, its evaluation can be very time consuming. An alternative to the MCMC methods is the generalized Polynomial Chaos Expansion (gPCE), which approximates the stochastic solution by a polynomial series.

The Bayesian Inference evaluates an updated distribution for the parameters of interest using the difference of experimental results and simulations to calculate the likelihood function. Marzouk and Xiu (2009) proposed the approximation of the simulation results by the gPCE. The authors evaluated the convergence rate and showed a numerical strategy to solve this type of problem. Nagel and Sudret (2016) proposed the approximation of the whole likelihood function by a polynomial series. The authors discussed the pros and cons of this approach being one advantage the simplification of the form of the parameters distribution, which is a product between a known probabilistic distribution and a polynomial series.

Wiener (1938) was the first to propose the approximation of stochastic process by a polynomial series. The author called "The Homogeneous Chaos", which approximated Gaussian processes by Hermite polynomials with satisfactory convergence. However, if the problem involves Non-Gaussian processes, the polynomial expansion may not converge. Xiu and Karniadakis (2002) expanded the idea of the Homogeneous Chaos for other polynomials families, which were in the Askey scheme. Therefore, Non-Gaussian processes can be approximated.

Thus, the stochastic problem become the evaluation of expansion coefficients. The Stochastic Collocation is a method that can evaluate the coefficients and its implementation is straightforward and simple. In this method, samples are evaluated and the coefficients are calculated by the Least Square method. Garoli *et al.* (2018) validated the use of the Stochastic Collocation to evaluate the expansion coefficients for the Bayesian Inference in order to identify unbalance parameters.

This work intends to separately identify the parameters of unbalance and misalignment faults by the Bayesian Inference via gPCE. Pseudo-experimental results are used to evaluate the application of the method. The Discrete Fourier

Transform (DFT) of the time response is performed and it is the input of the inference.

## 2. Rotor Model

In this work the rotor is modelled by the Finite Element Method. Shaft and journal are numerically represented by Timoshenko beam elements, in which each node has four degrees of freedom, two translational and two rotational, describing a planar analysis. Disc is modelled as rigid disc having concentrated mass and moment of inertia. Figure 1 shows the rotor used in the simulations.

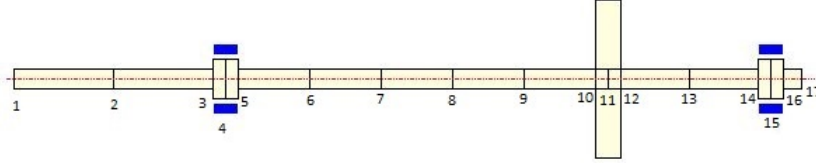


Figure 1. Mathematical model of the rotor.

Nodes 4 and 15 are the positions of hydrodynamic bearings that are used as rotor supports. The bearings are represented by the dynamic coefficients of damping and stiffness that are obtained by the solution of the isoviscous Reynolds equation (Lund, 1987).

Thus, it is possible to obtain the equation of motion, Equation 1:

$$\mathbf{M}\ddot{\mathbf{q}} + (\mathbf{C} + \mathbf{C}_b + \Omega\mathbf{G})\dot{\mathbf{q}} + (\mathbf{K} + \mathbf{K}_b)\mathbf{q} = \mathbf{F} \quad (1)$$

where,  $\mathbf{M}$ ,  $\mathbf{C}$ ,  $\mathbf{G}$  and  $\mathbf{K}$  are the mass, damping, gyroscopic and stiffness matrices of the rotor,  $\mathbf{C}_b$  and  $\mathbf{K}_b$  are the matrices containing the dynamic coefficients of damping and stiffness of the hydrodynamic bearings,  $\Omega$  is the spin speed,  $\mathbf{q}$  is the vector composed by all degrees of freedom for the rotating system, and  $\mathbf{F}$  is the external forces vector that can be due to unbalance  $\mathbf{F}_{\text{unb}}$  or misalignment  $\mathbf{F}_m$ .

This work considers the effect of mass unbalance and angular misalignment as the external forces, being mass unbalance the main cause of vibration in a rotating machinery, followed by misalignment (Patel and Darpe, 2009). The unbalance comes from the resultant inertial force of a residual mass  $m$  that is nonconcentric with the spin axis of the rotor by a distance  $e$ . As well known the unbalance force  $\mathbf{F}_{\text{unb}}$  can be written for the translational degrees of freedom as follows:

$$\mathbf{F}_{\text{unb}} = me\Omega^2 \begin{Bmatrix} \cos(\Omega t + \phi) \\ \sin(\Omega t + \phi) \end{Bmatrix} \quad (2)$$

which,  $\phi$  is the phase angle and  $t$  is the time variable.

On the other side, forces and moments arise in flexible couplings due to the accommodation of misalignment, being these efforts exerted on coupled shafts. The compliant element in a flexible disc coupling is the metallic disc. Here, the geometric relation between the thickness and the diameter of the disc is assumed 15/1000. The misalignment is compensated by bending of the disc segments between the bolts as can be seen in Figure 2(a), pointing to the suitability of plate elements to resist to loads normal to the disc surface, generating bending efforts. On the other hand, torque transmission in couplings generates tensile and compression stresses in the disc plane as Figure 2(b), indicating the usage of membrane elements to resist to load on the disc plane. Consequently, shell elements are used to model the disc component of the coupling, which combine membrane and plate effects (Tuckmantel and Cavalca, 2019).

Structural static analysis of the disc element is accomplished by Abaqus software using S4R quadrilateral shell element, and prescribed angular displacement are given as boundary conditions at the bolts position (see example in Figure 3). Moreover, spacer, bolts and hubs are discretized by three-dimensional solid element C3D8I.

For a given level of angular misalignment, successive shaft spin angles analysis lead to the cyclic nature of coupling efforts, adjusted by a fifth order polynomial equation through least squares method (Figure 4). Applied forces and moments in the driving hub as well as reaction forces and moments in the driven hub are extracted during the structural static analysis carried out in Abaqus. Therefore, the misalignment vector  $\mathbf{F}_m$  depends on the spin rotation  $\Omega$  and the angular misalignment  $\alpha$  (Tuckmantel and Cavalca, 2019).

## 3. Identification of the faults parameters

The Bayesian Inference is used to identify the fault parameters. It is a probabilistic method to update the probability density function of a random variable. Monte Carlo methods are commonly implemented to evaluate the solution of the inference. However, this methods can take a long processing time. It is proposed the use of the gPCE to approximate the likelihood function and the Stochastic Collocation method to evaluate the expansion coefficients.

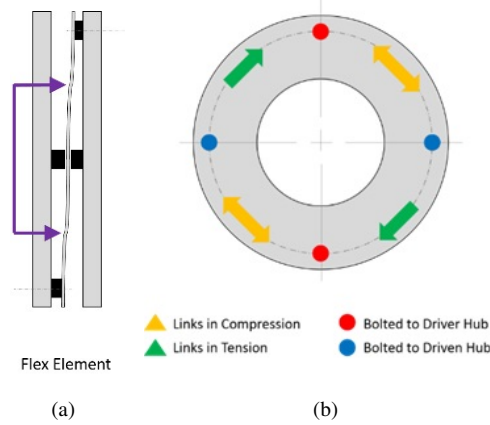


Figure 2. . Disc coupling (a) misalignment accommodation and (b) torque transmission Tuckmantel and Cavalca (2019)



Figure 3. Disc coupling.

### 3.1 Bayesian Inference

This inference method makes use of the Bayes Theorem, which allows the description of the probability distribution of an event  $\theta$  based on a previous knowledge about it and observations  $X$  related to it. Equation 3 presents the Bayes theorem,

$$p(\theta|X) = \frac{p(X|\theta) \cdot p(\theta)}{p(X)} = \frac{p(X|\theta) \cdot p(\theta)}{\int p(X|\theta) \cdot p(\theta)d\theta}, \quad (3)$$

in which  $p(\theta)$  is the priori distribution (what is known about the event),  $p(\theta|X)$  is the posteriori distribution, the updated distribution of the variable,  $p(X)$  is the probability of the observation happening, independent of  $\theta$ , and  $p(X|\theta)$  is the likelihood function, which is the propability observations given that  $\theta$  is known, given by Equation 4

$$p(X|\theta) = \exp(-k \cdot \sum_i^N \varepsilon_i^2), \quad (4)$$

with

$$\varepsilon_i^2 = \left( \sum_{i=1}^{ns} w_i (\sqrt{(Re(qe_i) - Re(qe_s))^2 + (Im(qe_i) - Im(qe_s))^2}) \right)^2, \quad (5)$$

with  $qe_i$  is the experimental results,  $qe_s$  as the simulation results,  $k$  is an arbitrary weight to adequate the likelihood function and  $w_i$  is a weigth to enrich more important parts of the results (for example: a specific frequency in the DFT).

### 3.2 Generalized Polynomial Chaos Expansion

It is proposed the approximation of the likelihood function by the gPCE. Therefore, a polynomial basis is constructed and the polynomials follow the orthogonal relation:

$$\langle \varphi_m, \varphi_n \rangle = \int \varphi_m(\theta) \cdot \varphi_n(\theta) \cdot p(\theta)d\theta = h_m^2 \cdot \delta_{mn} \quad (6)$$

with  $\delta_{mn}$  as the Kronecker delta and  $h_m^2 = \langle \varphi_m, \varphi_m \rangle$ . The polynomial families are related to the stochastic processes through the weigthing function  $p(\theta)$  in the orthogonality equation, which are similar to the probability density function of

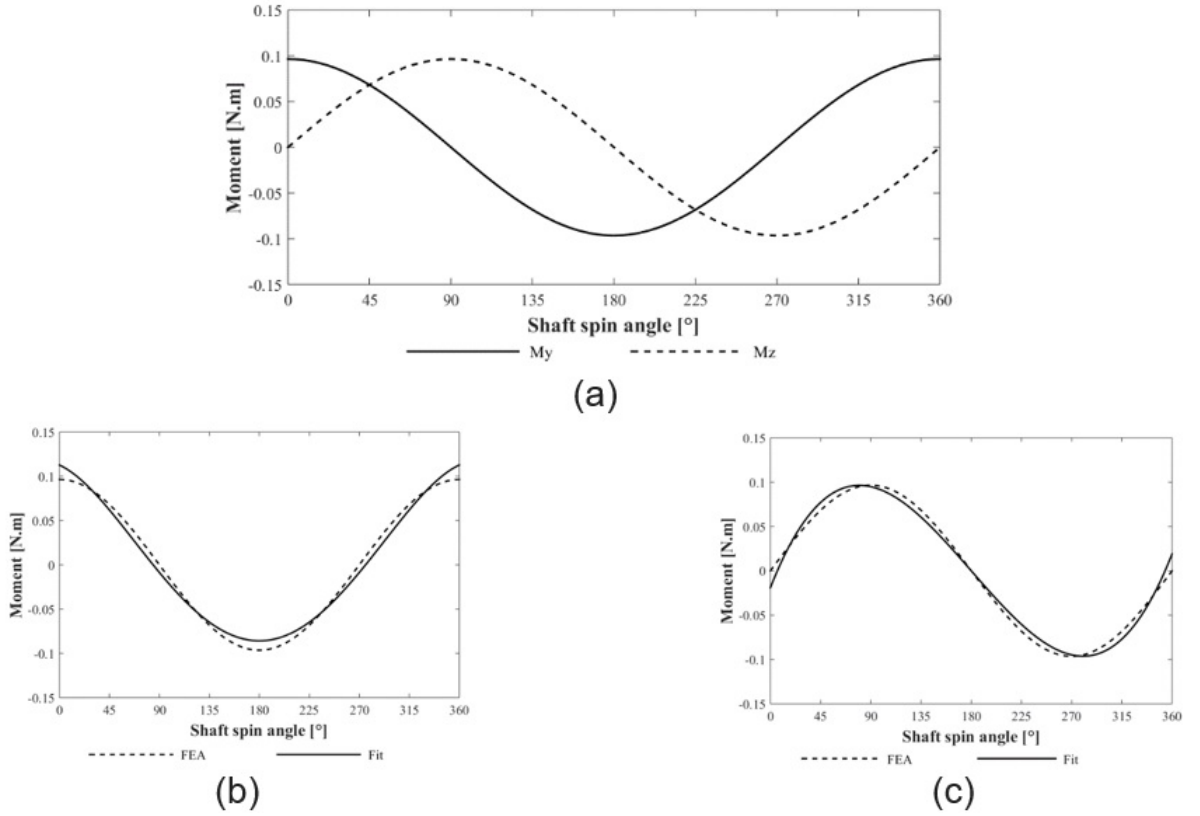


Figure 4. Coupling restoring (a) moments for  $0.5^\circ$  angular misalignment at 20Hz; calculated and adjusted moments (b)  $M_y$  and (c)  $M_z$ .

these processes.

Therefore, stochastic processes  $q(\theta, \lambda, t)$  can be approximated by a polynomial series, as presented in the Equation 7

$$q(\theta, \lambda, t) = \sum_{i=1}^M \hat{q}_i(\lambda, t) \cdot \varphi_i(\theta) \quad M = \binom{N+P}{N}, \quad (7)$$

with  $\theta$  as the random variables,  $\lambda$  as the non-random variables,  $t$  as time,  $N$  as the number of random variables and  $P$  as the maximum degree of the polynomials. In this way, the stochastic problem resumes into evaluating the expansion coefficients. To do that,  $Q$  samples of the random variables are made, then evaluated in a deterministic solver and used to solve the linear system presented by Equation 8

$$\begin{bmatrix} \varphi_1(\theta^1) & \cdots & \varphi_M(\theta^1) \\ \vdots & \ddots & \vdots \\ \varphi_1(\theta^Q) & \cdots & \varphi_M(\theta^Q) \end{bmatrix} \cdot \begin{Bmatrix} \hat{q}_1(\lambda, t) \\ \vdots \\ \hat{q}_M(\lambda, t) \end{Bmatrix} = \begin{Bmatrix} q(\theta^1, \lambda, t) \\ \vdots \\ q(\theta^Q, \lambda, t) \end{Bmatrix}. \quad (8)$$

### 3.3 Solving the Bayesian Inference

To solve the Bayesian Inference, the likelihood function is approximated by the gPCE. Therefore, the posteriori distribution becomes a product between a polynomial series and a known distribution, as presented in Equation 9.

$$p(\theta|X) = \frac{p_N^P(X|\theta) \cdot p(\theta)}{\int p_N^P(X|\theta) \cdot p(\theta) d\theta} \quad (9)$$

Due to the orthogonal properties of the polynomials, the integral can be solved as in Equation 10

$$\int p(X|\theta) \cdot p(\theta) d\theta = \int \sum_{i=1}^M (\hat{p}_i(X|\theta) \cdot \varphi_i(\theta)) \cdot 1 \cdot p(\theta) d\theta = \hat{p}_1(X|\theta). \quad (10)$$

Finally, the posteriori distribution form is

$$p(\theta|X) = \frac{p_N^P(X|\theta) \cdot p(\theta)}{\hat{p}_1(X|\theta)}. \quad (11)$$

Unlike MCMC methods, which generates a chain of each sample respecting the posteriori distribution, the evaluation of the Bayesian Inference by the gPCE is a function dependent on all the random variables. To improve the visualization of the distributions for each random variable, the marginal posteriori distribution must be evaluated. This can be made as shown in Equation 12

$$p(\theta_j|X) = \int p(\theta|X) d\theta_{\sim j} \approx \int \frac{p_N^P(X|\theta) \cdot p(\theta)}{\hat{p}_1(X|\theta)} d\theta_j = \frac{p_{N_j}^P(X|\theta_j) \cdot p_j(\theta_j)}{\hat{p}_1(X|\theta)} \quad (12)$$

in which  $\theta_{\sim j}$  are all random variables except  $\theta$ . Putting into words, the marginal posteriori distribution is all the terms of the gPCE that are dependent exclusively of  $\theta_i$ .

#### 4. Results

Two cases are considered for the numerical tests. In the first case, it is considered that the rotor system is subjected only to the unbalance fault and, in the second case, only the misalignment is considered. For both cases and for all faults parameters, it was considered uniform distribution as the priori knowledge and the DFT of the rotor system response was used as the experimental and simulation data.

For the first case, an unbalance moment of  $2 \cdot 10^{-4}$  kg.m at a phase of  $115^\circ$  was considered and located at node 11. The DFT of the response of the displacements in the bearing were considered as the experimental and simulated data for the construction of the likelihood function. Forty nodes were needed to approximate the likelihood function through the gPCE with maximum degree of the polynomial 8, with a total of 45 terms in the series. The inference was applied between nodes 9 and 13, so the position node could be determined.

Figures 5 to 9 present the marginal posteriori distribution evaluated for the unbalance moment and phase of the unbalance fault. In each figure, the expected values evaluated by the marginal posteriori distributions are presented by a \* in the horizontal axis and the values used to generate the experimental data are shown as a vertical line. There is a dot at the maximum probability.

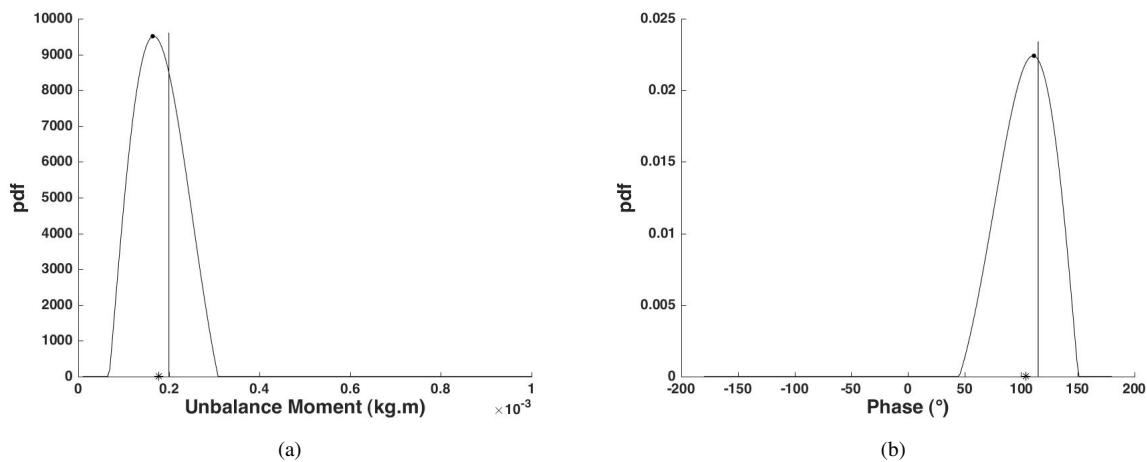


Figure 5. Marginal posteriori distribution of unbalance moment (a) and phase (b) at the node 9 (\* is the expected values and  $\cdot$  is the maximum probability value)

The expected values evaluated through the marginal posteriori distributions for each parameter are presented in Table 1. The values at node 11 are the closest to the real values. The growth of the expected values of the unbalance moment are due to the proximity with a bearing (in node 14). Therefore, a higher unbalance moment would be needed to reach the same vibration level of the experimental data.

Figure 10 presents the maximum probability of the phase at each node allowing the identification of the position node. The maximum probability is located at the node 12, which will be considered as the identified node in future simulations. Even though, the real position of the unbalance, node 11, has the second highest probability.

With the identified values of the node 12, the stochastic response of the system is evaluated. The maximum amplitude of the DFT and with the limits of the 95% confidence region for each bearing are presented in Table 4. The means of the stochastic response are close to the ones with the real values. Therefore, the identified parameters are satisfactory.

For the case of the unbalance fault, the Bayesian Inference with the gPCE approximation of the likelihood function can identify the values of the unbalance moment and the phase with expected values really close to the real values, if the

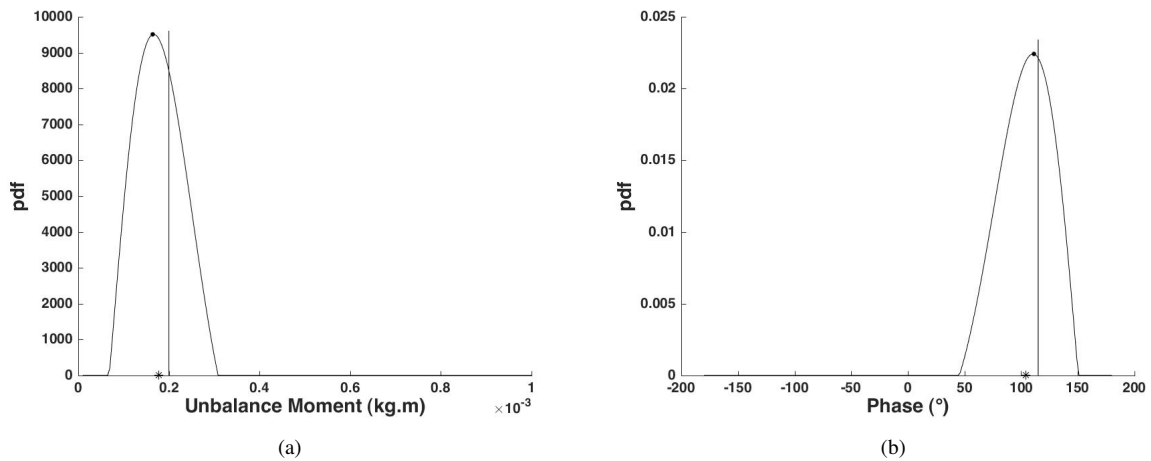


Figure 6. Marginal posteriori distribution of unbalance moment (a) and phase (b) at the node 10 (\* is the expected values and · is the maximum probability value)

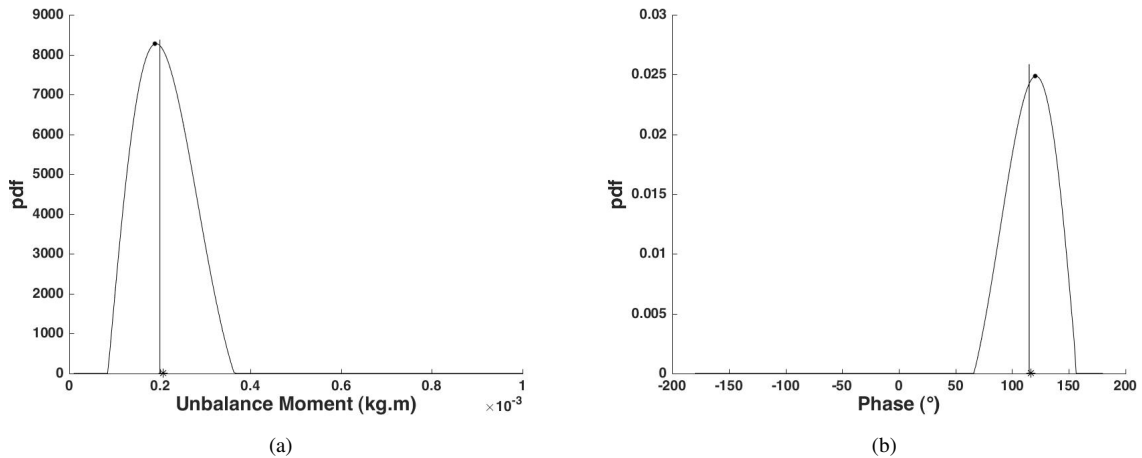


Figure 7. Marginal posteriori distribution of unbalance moment (a) and phase (b) at the node 11 (\* is the expected values and · is the maximum probability value)

Table 1. Mean of the identified parameter for each node

	Unbalance Moment ( $10^{-4}$ kg · m)	Phase (degree)
Real Value	2.0000	115.0000
Node 9	1.7771	104.3864
Node 10	1.7768	104.3167
Node 11	2.0753	116.3762
Node 12	2.1814	119.0129
Node 13	3.3157	120.2721

node where the unbalance is located is known. However, even when the method has to identify the position node, the method presents satisfactory results.

In the second case, the DFT of a rotor response subjected to a misalignment of  $0.2005^\circ$  and  $-0.5730^\circ$  was considered as the experimental data. To identify these parameters a polynomial expansion of 91 terms and maximum degree of 12 were used and 529 nodes were needed to evaluate the expansion coefficients.

Figure 11 shows the marginal posteriori distribution for each misalignment angle. The expected value for the angle 1 is 0.1858 and for the angle 2 is  $-0.5360$ , which are close to the values used to generate the experimental data. For the case of misalignment, the coupling is located in node 1 of the finite element discretization.

As expected values of the angles are close to the expected values used to evaluate the experimental data, the method can identify the fault parameters. Table 4 shows the amplitude responses with the real values and identified values for the misalignment angles, considering a confidence region of 95%. The influence of the uncertainties on the response in the

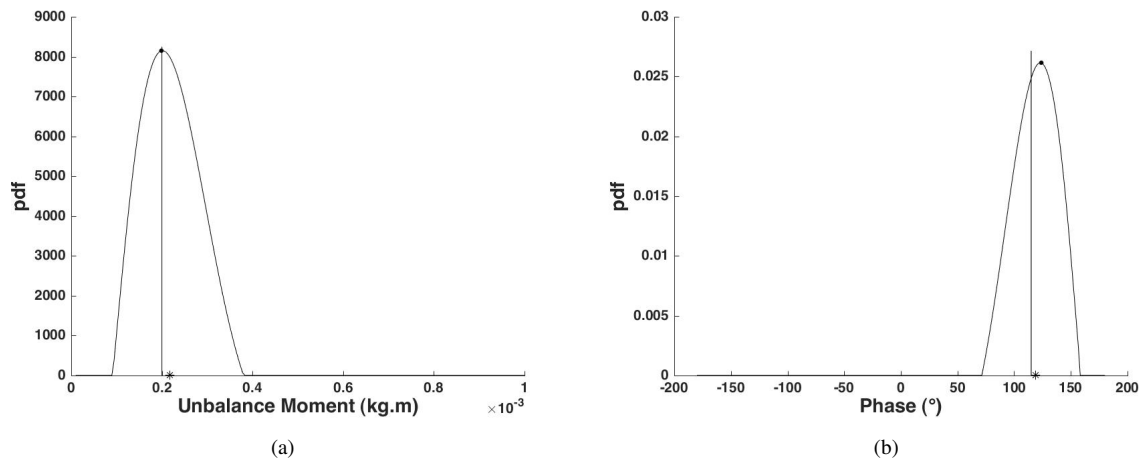


Figure 8. Marginal posteriori distribution of unbalance moment (a) and phase (b) at the node 12 (\* is the expected values and · is the maximum probability value)

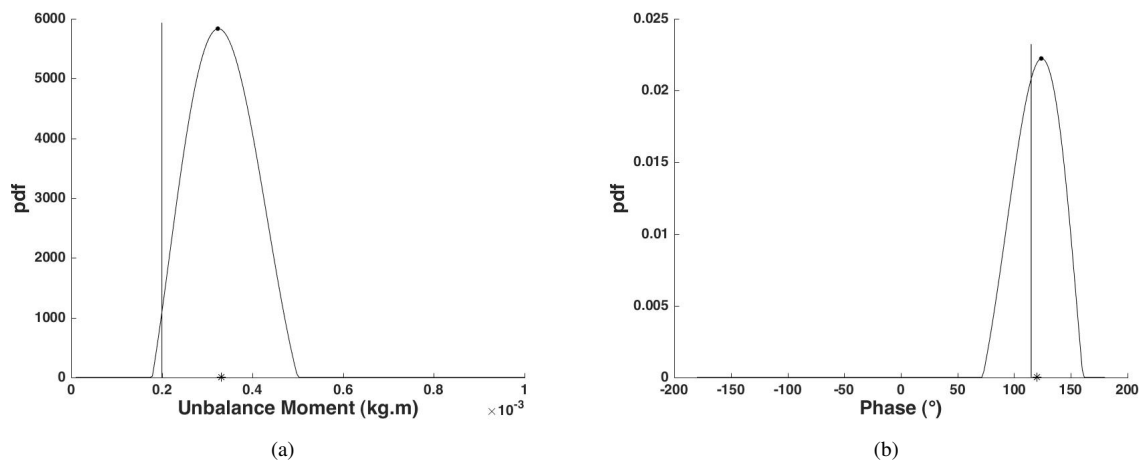


Figure 9. Marginal posteriori distribution of unbalance moment (a) and phase (b) at the node 13 (\* is the expected values and · is the maximum probability value)

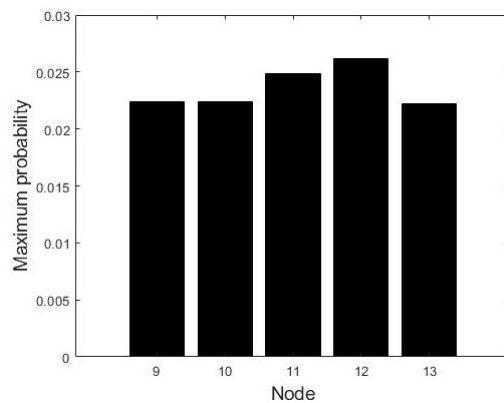


Figure 10. Maximum probability of the phase at each node

bearing 1 is higher than on the bearing 2, due to the proximity to the coupling. As the identified amplitudes are close the the expected values, it is possible to confirm the efficiency of the method.

## 5. Conclusion

In this work, the identification of the parameters of faults present in rotating machines was made. A rotor system in two different situations was considered. The first one, subjected to the unbalance fault and, the second one, subjected to

Table 2. Amplitude in the critical speed from the real and stochastic DFT (in $10^{-6}$  m)

Bearing	Real Value	Mean	[Inferior,Superior] Limits
1	8.6093	9.0623	[6.5535, 11.5713]
2	28.1279	27.9668	[20.2246, 35.7091]

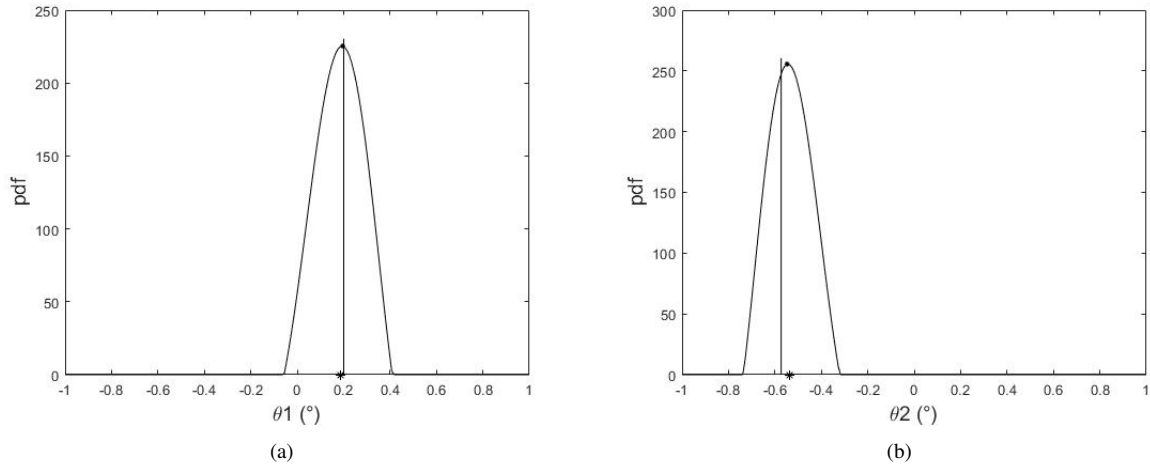


Figure 11. Misalignment with expected values of Angle1=0.57 degree (a) and Angle2=-0.57 degree (b) (\* is the expected values and · is the maximum probability value)

Table 3. Maximum amplitude of the time response (in $10^{-6}$  m)

Bearing	Real Value	Mean	[Inferior,Superior] Limits
1	0.4397	0.4176	[0.2442, 0.6269]
2	1.5396	1.5161	[1.4283, 1.6744]

the misalignment. For the unbalance fault, the unbalance moment, phase and the position node are the parameter to be identified. And for the misalignment, both angles are needed to the model.

The identification was held by the Bayesian Inference, which is commonly solved by Monte Carlo via Markov Chains methods. Depending on the deterministic solver, the evaluation of the posteriori function can take an unfeasible processing time. Therefore, the approximation by the generalized Polynomial Chaos Expansion of the likelihood function is proposed. This approximation resumes the evaluation of the posteriori distribution into the product between a polynomial series and a known probability distribution.

The method identified the parameters for the case of the unbalance with known position node and the angles of the misalignment, with expected values close to the real ones. When the position node was unknown, the method evaluated satisfactory expected values for the unbalance moment and phase.

## 6. ACKNOWLEDGEMENTS

The authors would like to thank FAPESP (grant# 2015/20363-6 and grant#2016/13223-6) for the financial support of this research.

## 7. REFERENCES

- Garoli, G.Y., Tyminski, N.C. and de Castro, H.F., 2018. "Stochastic collocation approach to bayesian inference applied to rotating system parameter identification". In *Proceedings of the 10th International Conference on Rotor Dynamics - IFToMM2018*. Vol. 4, pp. 401-415.
- Lund, J.W., 1987. "Review of the concept of dynamic coefficients for fluid film journal bearings". *Journal of Tribology*, Vol. 109, No. 1, pp. 37-41.
- Marzouk, Y. and Xiu, D., 2009. "A stochastic collocation approach to bayesian inference in inverse problems". *Communications in Computational Physics*, Vol. 6, No. 4, pp. 826-847.
- Nagel, J.B. and Sudret, B., 2016. "Spectral likelihood expansions for bayesian inference". *Journal of Computational Physics*, Vol. 309, pp. 267-294.
- Patel, T. and Darpe, A., 2009. "Vibration response of misaligned rotors". *Journal of Sound and Vibration*, Vol. 325, pp.

609–628.

Tuckmantel, F.W.S. and Cavalca, K.L., 2019. “Vibration signatures of a rotor-coupling-bearing system under angular misalignment”. *Mechanism and Machine Theory*, Vol. 133, pp. 559–583.

Wiener, N., 1938. “The homogeneous chaos”. *American Journal of Mathematics*, Vol. 60, No. 4, pp. 897–936.

Xiu, D. and Karniadakis, G., 2002. “The wiener–askey polynomial chaos for stochastic differential equations”. *SIAM Journal of Scientific Computing*, Vol. 24, No. 2, p. 619–644.

## **8. RESPONSIBILITY NOTICE**

The authors are the only responsible for the printed material included in this paper.